# Simulation of conventional porosity well logging obtained from the mineral distribution data of carbonate core.

Giulia Lima Ciabotti, Rodrigo Bagueira de V. Azeredo, Alfredo M.V. Carrasco UFF/TEQ - Niterói, RJ



## Abstract

Information coming from different porosity systems in carbonate reservoirs is of great importance in reservoir engineering and rock petrophysics.
In this study, we use the information of carbonate samples (plugs), representing some porosity systems, such as intercrystalline, intergrain, moldic, vuggy and fracture. Porosity was measured as fraction and mineralogy due to the presence of clay, quartz, feldspar, carbonate, anhydrite and iron. With this information, we used an algorithm developed to simulate the responses of conventional porosity well logging based on the mineral content of different samples when the pore system is occupied by water.
Porous system in carbonate formation are more complex than clastic formation, because carbonates are a mixture of some porous systems as intercrystalline, moldic, intergrain, vuggy and all of them within a matrix. The quantitative porosity values is difficult to calculate, so these features were defined qualitatively for each sample. Thus, to simulate the porosity responses, we took as reference their radioactive and acoustic properties of the minerals as well as their percentage.

## Introduction

Theoretical models based on the physics of rocks sets relationships between the porous structure and the elastic, radioactive and electrical properties. Although significant progress has happened in inverse modeling problems about porous structure obtained from physical properties of rock, factors as multiplicity of responses, computational stability and availability of core analysis information, limits their reliable petrophysical characterization (Wu & Chen, 2014). Therefore the aim of this work is the forward modeling, based on the mineralogy data taken from different carbonate samples and their petrophysical properties. In the simulation it was considered the pore system filled only with water, to avoid the influence on responses when the porous system is occupied by hydrocarbons.

In the simulation was not included the effect of the drilling fluid invasion process, because it is a one-dimensional system. To get the responses, we considered a lithology with three layers, a carbonate layer located between two shales layers. To simulate the shale layers, it was taken as reference the clay mineral characteristics found in the carbonates layers as well as their radioactivity characteristics. For the carbonate layers we considered a set of 2 or 3 layers of a representative pore system, which will be detailed in the methodology.

The minerals in calcareous rocks are mainly calcite ($CaCO_3$), aragonite ($CaCO_3$ - same chemical composition of calcite, but with different structure) and dolomite ($CaMg(CO3)_2$). Calcite, aragonite and dolomite differ considerably in their solubility and sedimentology. Thus, aragonite is more soluble than aragonite and calcite (Schlager, 2005). It is believed that the best reservoirs are located in areas with large amounts of dolomite, because their presence could be associated with the increased of secondary porosity (vuggs and fractures) (Miranda et al, 2008).

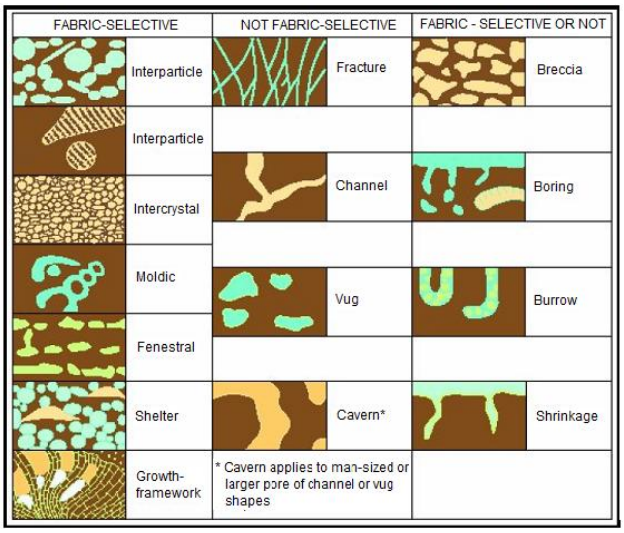


Figure 1. The carbonate porosity classification (Choquette & Pray, 1970)

Other minerals may be present, as defined in the samples, such as clays, quartz, feldspar, anhydrite and iron.

To establish a classification of the carbonates porosities, Choquette - Pray (1970) recognized the need to include the period and their origin in the description. They considered 15 types of pores arranged in three classes dependent on the fabric, as shown in Figure 1. The porosity with selective fabric can be depositional, diagenetic or both of them. No selective fabrics include fractures or cavities formed by dissolution process. Fabric selective or not, is a category that includes animal or plants characteristics or from erosion or tectonic process (Ahr, 2008). Lucia

(1995), established another classification in 1983, making a division between two types of porosities: intergrain (Figure 2) and moldic (isolated or connected by microfractures).

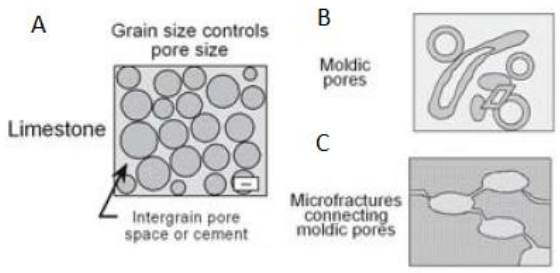


Figure 2. Porosity classification by Lucia (modified Lucia, 2004)

This classification also has a division, since the intergrain porosity would have a fabric mainly with grains (Figure 2A) or having a mud fabric. Likewise, the vuggy porosity without connection can be moldic (Figure 2B), intrafossil or intragrain. The subdivision for the connected vugular porosity can be: cave type, fracture, fractures extended by dissolving processes, fenestral, or moldic with microfractures interconnection (Figure 2C), (Lucia, 2004).

**Method**

Samples to be used in this work are classified according to the type of rock and porosity, and were divided into 5 groups as shown in following tables. Thus, Table 1 corresponds to a chalk sample with intercrystalline and intergranular porosity:

Table 1. Chalk with Intercrystalline and Intergranular porosity

| sample | porosity | shale | quartz | feldspar | carbonate | anhydrite | iron |
|---|---|---|---|---|---|---|---|
| CH13 | 0,019 | 0,415 | 0,235 | 0,155 | 0,131 | 0,041 | 0,005 |
| CH21 | 0,018 | 0,379 | 0,236 | 0,181 | 0,161 | 0,024 | 0,001 |
| CH22 | 0,019 | 0,347 | 0,209 | 0,170 | 0,204 | 0,049 | 0,001 |

Table 2 also corresponds to chalk with intergranular and, intercrystalline porosity but including fracture porosity. Samples from these two tables correspond to the North Sea (Norway).

Table 2. Chalk with Intercrystalline, Intergranular and fracture porosity

| sample | porosity | shale | quartz | feldspar | carbonate | anhydrite | iron |
|---|---|---|---|---|---|---|---|
| CH013 | 0,021 | 0,262 | 0,16 | 0,17 | 0,349 | 0,038 | 0 |
| CH014 | 0,018 | 0,304 | 0,189 | 0,171 | 0,266 | 0,052 | 0,001 |

Table 3 data corresponds to the region of Abu Dhabi and they are diagenetic chalk with intercrystalline, moldic and intergranular porosity.

Table 3. Diagenetic Chalk with Intercrystalline, moldic and Intergranular porosity

| sample | porosity | shale | quartz | feldspar | carbonate | anhydrite | iron |
|---|---|---|---|---|---|---|---|
| DC11 | 0,023 | 0,167 | 0,125 | 0,24 | 0,405 | 0,039 | 0 |
| DC12 | 0,024 | 0,169 | 0,124 | 0,206 | 0,437 | 0,04 | 0 |
| DC13 | 0,013 | 0,181 | 0,161 | 0,201 | 0,389 | 0,053 | 0,001 |

The microcrystalline dolomite from Table 4 shows intercrystalline and moldic porosity and corresponds to the Texas region (USA).

Table 4. Microcrystalline Dolomite with Intercrystalline and moldic porosity

| sample | porosity | shale | quartz | feldspar | carbonate | anhydrite | iron |
|---|---|---|---|---|---|---|---|
| MD11 | 0,075 | 0,058 | 0,024 | 0,162 | 0,659 | 0,022 | 0 |
| MD12 | 0,15 | 0,088 | 0,029 | 0,106 | 0,573 | 0,053 | 0 |
| MD13 | 0,128 | 0,083 | 0,022 | 0,093 | 0,643 | 0,031 | 0 |

Finally, the data in Table 5, belong to an oolitic limestone with intergrain porosity and dissolved grains. They are from Tunisia.

Table 5. Oolitic Limestone with intergrain porosity and dissolved grains

| sample | porosity | shale | quartz | feldspar | carbonate | anhydrite | iron |
|---|---|---|---|---|---|---|---|
| VD22 | 0,135 | 0,046 | 0,021 | 0,168 | 0,535 | 0,094 | 0,001 |
| VD23 | 0,11 | 0,023 | 0,021 | 0,173 | 0,603 | 0,069 | 0 |
| VD31 | 0,071 | 0,023 | 0,017 | 0,177 | 0,676 | 0,036 | 0 |

For each of these data shown in the tables above, the responses simulated corresponds to the following logs: gamma ray, density, neutron and sonic.

The program simulates their responses based on their characteristic acoustic, radioactive, capture cross section and density values for each mineral. In some cases these values are not unique, as shown in the following table:

| | | quartz | carbonate | anhydrite | shale | feldspar | iron |
|---|---|---|---|---|---|---|---|
| potassium | K min | 0 | 0 | 0 | 0 | 0 | 0 |
| barn/cc | Kmax | 0,15 | 0,1 | 8,48 | 1,69 | 15 | 0 |
| uranium | U min | 0 | 0 | 0 | 0,24 | 0,2 | 0 |
| barn/cc | U max | 0,4 | 1 | 0,35 | 3,17 | 2 | 0 |
| thorium | T min | 0 | 0 | 0 | 1,67 | 0 | 0 |
| barn/cc | T max | 0,2 | 0,5 | 0,1 | 20,7 | 3 | 0 |
| density | (gr/cc) | 2,65 | 2,71-3,89 | 2,98 | 2,12-2,76 | 2,52-2,59 | 4,53-4,99 |
| transit t. | (us/ft) | 51,0-55,5 | 43,5-47,6 | 50 | 62,4-167,0 | 69 | 39,2 |
| cross sec | (sigma,cu) | 4,26 | 7,08-52,31 | 12,45 | 14,12-24,87 | 15,51-15,58 | 90,1 |

Tabela 6. Characteristic values of minerals (Johnson & Pile, 2006)

To simulate the log responses was selected an initial value for each of the minerals shown in Table 6, as data entry to the algorithm. The algorithm will simulate the responses of porosity logs on the basis of these data, which must be close to the sample porosity value. If there is a significant difference, we will change some values used. Thus, we selected the most representative values of mineralogy for each region (North Sea, Abu Dhabi, Texas, and Tunisia).

The values of the Gamma Ray log (GR) were obtained on the basis the clay content present in the carbonates, because we have not representative samples for shale from the region. In all cases was simulated profile one lithological sequence of shale - carbonate - shale.

**Results**

The first group of profiles of Figure 3 corresponds to the simulated data set shown in Table 1.

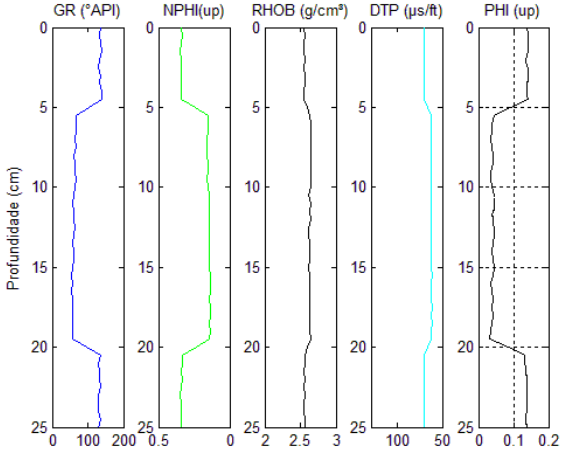


Figura 3. Chalk – North Sea
(samples CH13 – CH21 – CH22)

In this group of simulated logs: gamma ray (GR), neutron (NPHI), density (RHOB) and sonic (DTP), were used three lithologic groups: shale - carbonate - shale. The shale layers correspond to upper and lower layers (0-5 cm and 20-25 cm). The response of carbonates was divided into three parts for the different samples of limestone CH13 (5-10 cm) CH11 (10-15 cm) and CH22 (15-20 cm) and located between the shales. Depth units were considered in centimeters, because of the rock samples (plugs). The last log (total porosity PHI) of Figure 3 is the result of the interaction of simulated NPHI and RHOB logs responses, and this value was approximate to the values of porosity sample (Table 1), after making several changes of the mineralogical values from Table 6. Table 7 shows the results for the group of chalks with intergrain and intercrystalline porosity from the North Sea region.
As can be seen in Table 7, Table 6 was taken as reference values to describe some of the parameters used to determine the theoretical porosity PHI (up) shown in Figure 3. This theoretical value of the total porosity was compared with the given value, as shown in Tables 1 to 5.

Similarly, with the same data was simulated for this region two groups of samples CH013 (5-10 cm) and CH014 (10-15cm) at depths indicated as shown in Figure 4. It is also observed that there are no differences between these results of Figures 3 and 4, since they are of the same kind and the same lithological type. The main difference is that limestone in Figure 4 has fracture porosity, in addition to intergrain and intercrystalline porosity. Because of the lack of reference about lithological information of shale, were assumed low values in the content of potassium, uranium and thorium. Units are the following: radioactivity in Barn / cc units, density in g / cc, transit time in us / ft and cross section in units capture (Cu), where 1c.u. = $10^{-3}$ $cm^2$ / $cm^3$.

The next simulation was used another group of samples (diagenetic chalk with intercrystalline, moldic and intergranular porosity), from the region of Abu Dhabi, as shown in Figure 5. Because of the diagenetic chalk, can be observed lower porosity values, compared to the North Sea chalk.

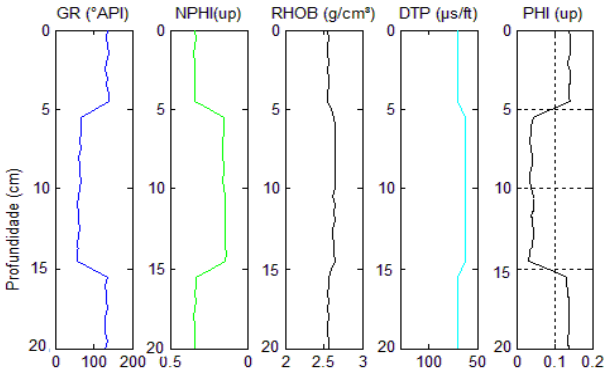


Figure 4. Chalk – North Sea
(samples CH013 – CH014)

| | quartz | carbonate | anhydrite | shale | feldspar | iron |
|---|---|---|---|---|---|---|
| potassium | 0,1 | 0,1 | 0,1 | 1,69 | 8,5 | 0 |
| uranium | 0,2 | 0,4 | 0,35 | 3,17 | 1,5 | 0 |
| thorium | 0,1 | 0,5 | 0,1 | 20,7 | 0,1 | 0 |
| density | 2,64 | 2,71 | 2,98 | 2,64 | 2,59 | 4,8 |
| transit t | 55,5 | 47,5 | 50 | 64,3 | 69 | 39,2 |
| cross sec. | 4,26 | 24,5 | 12,45 | 20,5 | 15,51 | 90,1 |

Table 7 Mineralogical characteristics of the North Sea Chalk

As a result of this simulation we obtained the values of Table 8. In this table we see that the parameters used are very similar to those in Table 7 because it is also chalk.

| | quartz | carbonate | anhydrite | shale | feldspar | iron |
|---|---|---|---|---|---|---|
| potassium | 0,1 | 0,1 | 0,1 | 1,69 | 8,5 | 0 |
| uranium | 0,2 | 1 | 0,35 | 3,17 | 1,5 | 0 |
| thorium | 0,1 | 0,5 | 0,1 | 20,7 | 0,1 | 0 |
| density | 2,64 | 2,71 | 2,98 | 2,64 | 2,59 | 4,8 |
| transit t | 55,5 | 48 | 50 | 64,3 | 69 | 39,2 |
| cross sec. | 4,26 | 24,5 | 12,45 | 20,5 | 15,51 | 90,1 |

Table 8. Mineralogical characteristics of diagenetic chalk of Abu Dhabi

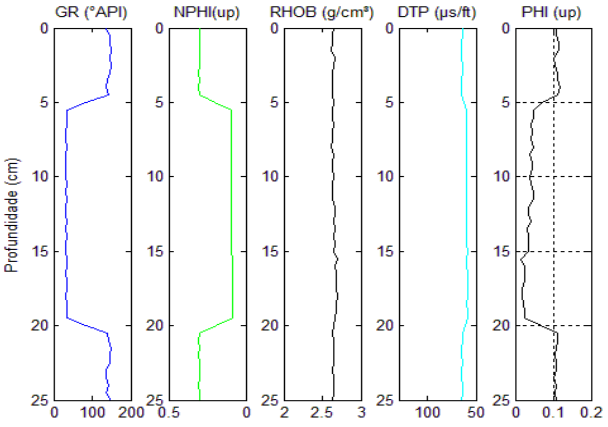


Figure 5. Diagenetic chalk – Abu Dhabi
(samples DC11 – DC12 – DC13)

Figure 6 shows the simulation results of microcrystalline dolomite with intercrystalline and moldic porosity. Each sample is referenced in depth function: MD11 (5-10cm), MD12 (10-15 cm) and the MD13 (15-20 cm) sample. The clay content of these samples is very low, which is reflected in the low values of the simulated GR log. For this simulation we use the following mineral values shown in Table 9.

| | quartz | carbonate | anhydrite | shale | feldspar | iron |
|---|---|---|---|---|---|---|
| potassium | 0,15 | 0,1 | 0,1 | 1,69 | 8,5 | 0 |
| uranium | 0,4 | 0,8 | 0,35 | 3,17 | 1,5 | 0 |
| thorium | 0,2 | 0,2 | 0,1 | 20,7 | 0,1 | 0 |
| density | 2,64 | 2,71 | 2,98 | 2,64 | 2,59 | 4,8 |
| transit t | 55,5 | 43,5 | 50 | 64,3 | 69 | 39,2 |
| cross sec. | 4,26 | 26,5 | 12,45 | 20,5 | 15,51 | 90,1 |

Table 9. Mineralogical Characteristc of Microcrystalline dolomite of Texas

In Table 9 were made changes in relation to transit time and capture units of the cross section of dolomite, as well as some changes in radioactivity values of clays.

Finally, we made a simulation using data of Table 5, which corresponds to a set of samples of oolítico limestone with intergrain porosity and dissolved grains, as shown in Figure 7. In this figure was observed low limestone radioactivity values for the three kinds of samples indicated. After several simulations we get the values shown in Table 10

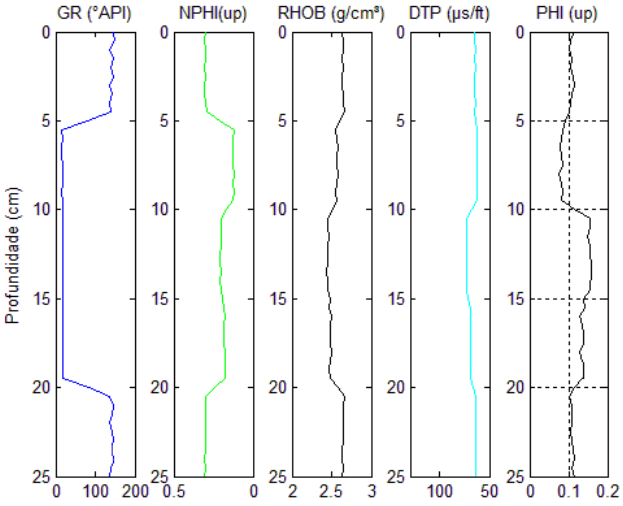


Figure 6. Microcrystalline Dolomite – Texas
Samples MD11- MD12 – MD13

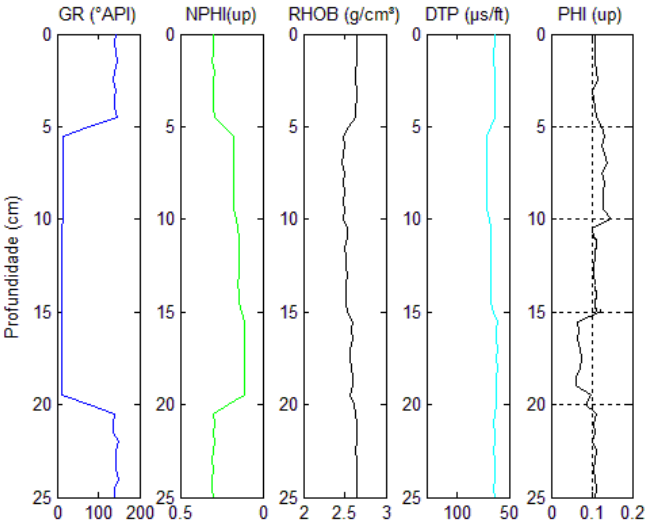


Figure 7. Oolitic Limestone – Tunisia
Samples VD22 – VD23 – VD 24

| | quartz | carbonate | anhydrite | shale | feldspar | iron |
|---|---|---|---|---|---|---|
| potassium | 0,1 | 0,1 | 0,1 | 1,69 | 8,5 | 0 |
| uranium | 0,2 | 1 | 0,35 | 3,17 | 1,5 | 0 |
| thorium | 0,1 | 0,5 | 0,1 | 20,7 | 0,1 | 0 |
| density | 2,64 | 2,71 | 2,98 | 2,64 | 2,59 | 4,8 |
| transit t | 55,5 | 48,5 | 50 | 64,3 | 69 | 39,2 |
| cross sec. | 4,26 | 24,5 | 12,45 | 20,5 | 15,51 | 90,1 |

Table 10. Mineralogical Characteristic of Oolitic Limestone - Tunisia

In Table 11 we can find the porosity values of each group of minerals obtained after the simulation process. To validate the mineralogical values, it was calculated the error percentage between the porosity calculated by the program and the porosity provided for each sample, as shown in Table 11.

| Sample | ø (data) | ϕ (calc) | erro (%) |
|---|---|---|---|
| CH13 | 0,019 | 0,019 | 0,00 |
| CH21 | 0,018 | 0,019 | 0,06 |
| CH22 | 0,019 | 0,019 | 0,00 |
| CH013 | 0,021 | 0,019 | 0,10 |
| CH014 | 0,018 | 0,019 | 0,06 |
| DC11 | 0,023 | 0,024 | 0,04 |
| DC12 | 0,024 | 0,023 | 0,04 |
| DC13 | 0,013 | 0,014 | 0,08 |
| MD11 | 0,075 | 0,080 | 0,07 |
| MD12 | 0,150 | 0,155 | 0,03 |
| MD13 | 0,128 | 0,130 | 0,02 |
| VD22 | 0,135 | 0,134 | 0,01 |
| VD23 | 0,110 | 0,111 | 0,01 |
| VC31 | 0,071 | 0,072 | 0,01 |

Table 11. Porosity values and error percentage

## Conclusions

The use of inverse modeling in order to calculate the carbonate porosity, has been studied with certain restrictions due to the ambiguity in their response. Using forward modeling, this ambiguity is low, because there are still some mineralogical parameters covering a range of values as shown in Table 6.

To validate this study about the relationship between porosity and mineralogy, we use the porosity calculated by the simulation program and that porosity provided by the samples. However the wide variety of parameters involved requires some geological knowledge of the area. Likewise, identifying the different types of porosity with the calculated porosity data is difficult task. However this study allows us to evaluate the behavior of the answers of porosity log, if we replace a hydrocarbon, liquid or gaseous fluids, instead of water.

## Acknowledgement

To the Federal Fluminense University (UFF) by infraestructure. ANP (Commitment to Investment in Research and Development) and BG Brazil for the data given and financial support

## References

Ahr, Wayne. 2008. Geology of Carbonate Reservoirs. The identification, description, and characterization of hydrocarbon reservoirs in carbonate rocks. Wiley Publication.

ART, Applied Reservoir Technology. The ResLab Group. 1997. The NMR Carbonate Rock Catalogue.

Choquette, P.W., Pray, L.C., 1970. Geologic Nomenclature and Classification of Porosity in Sedimentary Carbonates, AAPG Bulletin, v.54, p. 207-250.

Johnson, D. E. & Pile K. E. 2006. Well Logging in Nontechnical Language. Pennwell

Lucia, F.J. 2004. Carbonate Reservoir Characterization - An Integrated Approach, 2nd edition, 336p.

MATLAB. 2010. User´s Manual.

Miranda, L. J., Verdin C. T. & Lucia J. 2008. Modeling Mud-Filtrate Invasion Effects on Resistivity Logs to Estimate Permeability of Vuggy and Fracture Carbonate Formations, SPE.

Schlager, Wolfgang. 2005. Carbonate Sedimentology and sequence stratigraphy. Society for Sedimentary Geology.

Wu, Baohai & Chen, Liping. 2014. Optimizing calculation of multiple porosities in carbonates with petrophysics and rock physics integration strategy. SEG-2014-0906.